XV International Conference on Computational Plasticity. Fundamentals and Applications
COMPLAS 2019
E. Oñate, D.R.J. Owen, D. Peric, M. Chiumenti & Eduardo de Souza Neto (Eds)

ELASTIC PROPERTIES OF ISOTROPIC DISCRETE SYSTEMS WITH SKEW CONTACT NORMALS

JAN ELIÁŠ*

* Brno University of Technology
Faculty of Civil Engineering
Institute of Structural Mechanics
Veveří 331/95, Brno, 60200, Czech Republic
e-mail: jan.elias@vut.cz

Key words: Discrete model, homogenization, elasticity, Poisson's ratio, normal vector

Abstract. The macroscopic elastic properties of discrete assemblies are fundamental characteristics of such systems. The contribution uses homogenization procedure based on equivalence of virtual work between the isotropic elastic continuum and the discrete system to develop analytical formulas for estimation of macroscopic elastic modulus and Poisson's ratio.

Such homogenization was recently used to derive formulas for discrete assemblies where (i) there is no vacant space between the discrete units, (ii) the orientation of contacts is uniformly distributed and (iii) the contact normals are parallel to contact vectors (directions connecting centers of discrete units). The third assumption is now removed, three dimensional systems with arbitrary relation between contact vectors and contact normals are studied here.

It is shown that the limits of Poisson's ratio of such system depends on the relation between contact normal and contact vector. The widest limits are however obtained when these two vectors are parallel. This means that arbitrary manipulations with discrete geometry cannot extend Poisson's ratio of the system outside the known boundaries.

1 INTRODUCTION

Discrete modeling allows to explain or predict complex behavior of heterogeneous, cohesive or granular materials. It represents material random heterogeneity and also directly works with discrete and oriented nature of cracks. Its elastic behavior still posses open challenges. Besides the minor issue of inevitable boundary layer [1], the major problem lies in inability to exhibit Poisson's ratios greater than 1/4 for three dimensional models. The usage of the discrete models is therefore limited to materials with relatively low Poisson's ratio.

This paper is motivated by long belief of the author that Poisson's ratio of discrete systems can be increased by changing model geometry. Models described in literature

usually use contact faces between discrete units perpendicular to contact vectors [2, 3]. This restriction is here abandoned allowing to construct model of completely arbitrary geometry. Poisson's ratio is then analyzed using strong assumptions about rotations and translations in the model according to [4]. The paper unfortunately proves that geometrical changes lead only to shrinking of the interval of achievable Poisson's ratios. The previously published results derived for 2D models [5] are extended here into 3D.

The studied system is composed of ideally rigid bodies filling a domain continuously without gaps or overlapping. It is assumed that the system is isotropic in statistical sense – there is no directional dependence. The rigid bodies interact at their borders, where normal and tangential displacement discontinuities $\boldsymbol{\Delta}$ results in normal and tangential forces. Critical parameter governing the macroscopic Poisson's ratio is the ratio between tangential and normal contact stiffness denoted α hereinafter.

Equations are derived from virtual work equality between the discrete system and Boltzmann continuum subjected to equal straining. The discrete system yields non-symmetric stress tensor on contrary to the Boltzmann continuum symmetric stress quantity. The virtual work equivalence is therefore accomplished with help of symmetrization of the tensor of elastic constants from the discrete model. To simplify the notation, we introduce operation transposition T_{ij} on arbitrary tensor $\boldsymbol{A}$ of sufficient order by swapping indices i and j.

$$A^{T_{ij}}_{\ldots i\ldots j\ldots} = A_{\ldots j\ldots i\ldots} \tag{1}$$

2 FUNDAMENTAL GEOMETRIC RELATIONS

Each if the rigid bodies have 6 degrees of freedom associated with translations and rotations of some inner node, $\boldsymbol{x}_a$. The contact element between two nodes $\boldsymbol{x}_a$ and $\boldsymbol{x}_b$ has contact area A, length l, unit normal vector $\boldsymbol{n}$ and contact vector $\boldsymbol{t}$. The situation is sketched in Fig. 1a in two dimensions.

The vector $\boldsymbol{n}$ is here defined in Cartesian coordinate system by two angles, ξ and ζ

$$\boldsymbol{n} = (\cos\xi \sin\zeta,\ \sin\xi \sin\zeta,\ \cos\zeta) \tag{2}$$

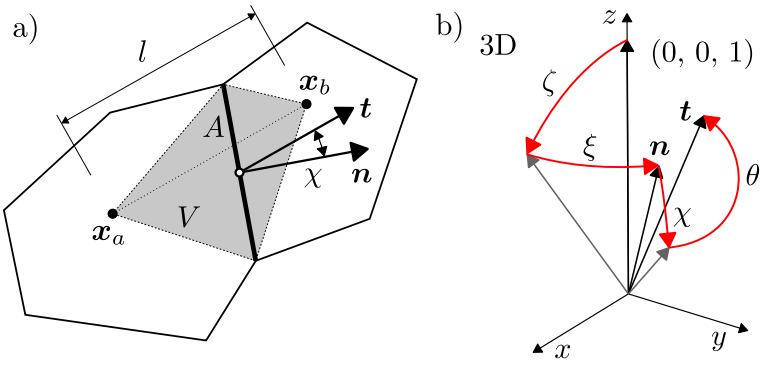

Figure 1: a) Contact between two rigid bodies, its normal and contact vector, area and volume; b) angles determining directions of normal and contact vector.

where ζ is angle between z axis and normal and ξ is the rotation of $\boldsymbol{n}$ around the z axis - see Fig. 1. We assume that the system has no directional bias, therefore all normal directions share the same probability of occurrence. Therefore, ξ must be uniform over interval from 0 to 2π and ζ has the following probability density function

$$f_\xi(\xi) = \begin{cases} \dfrac{1}{2\pi} & \text{for } \xi \in (0, 2\pi) \\ 0 & \text{otherwise} \end{cases} \qquad f_\zeta(\zeta) = \begin{cases} \dfrac{\sin\zeta}{2} & \text{for } \zeta \in (0, \pi) \\ 0 & \text{otherwise} \end{cases} \tag{3}$$

The contact vector $\boldsymbol{t}$ is defined relatively to normal vector $\boldsymbol{n}$ by angles χ and θ - see Fig. 1b. To ensure isotropic, directionally unbiased 3D structure θ is required to be uniformly distributed over 0–2π interval, probability distribution of f_χ can be arbitrary.

$$f_\theta(\theta) = \begin{cases} \dfrac{1}{2\pi} & \text{for } \theta \in (0, 2\pi) \\ 0 & \text{otherwise} \end{cases} \tag{4}$$

For sake of simplicity, it will be assumed now that the maximum angle between $\boldsymbol{n}$ and $\boldsymbol{t}$ is $\gamma \in (0,\ \pi)$ and all directions within this range are equally probable.

$$f_\chi(\chi) = \begin{cases} \dfrac{\sin\chi}{1-\cos\gamma} & \text{for } \theta \in (0, \gamma) \\ 0 & \text{otherwise} \end{cases} \tag{5}$$

Rotation matrix is the second order tensor that provides the following relation between $\boldsymbol{n}$ and $\boldsymbol{t}$

$$\boldsymbol{t} = \boldsymbol{R} \cdot \boldsymbol{n} \tag{6}$$

One can imagine construction of $\boldsymbol{n}$ via taking the vector $\begin{pmatrix} 0 & 0 & 1 \end{pmatrix}$, rotate it along the y axis by angle ζ and then along z axis by angle ξ (Fig. 1b). In the same way, the construction of $\boldsymbol{t}$ is done by four successive rotations along axes y, z, y and z by angles χ, θ, ζ and ξ, respectively.

$$\boldsymbol{n} = \boldsymbol{R}_z(\xi) \cdot \boldsymbol{R}_y(\zeta) \cdot \begin{pmatrix} 0 & 0 & 1 \end{pmatrix} \quad \boldsymbol{t} = \boldsymbol{R}_z(\xi) \cdot \boldsymbol{R}_y(\zeta) \cdot \boldsymbol{R}_z(\theta) \cdot \boldsymbol{R}_y(\chi) \cdot \begin{pmatrix} 0 & 0 & 1 \end{pmatrix} \tag{7}$$

The rotation matrix from Eq. (6) is therefore

$$\boldsymbol{R}(\xi, \zeta, \chi, \theta) = \boldsymbol{R}_z(\xi) \cdot \boldsymbol{R}_y(\zeta) \cdot \boldsymbol{R}_z(\theta) \cdot \boldsymbol{R}_y(\chi) \cdot \boldsymbol{R}_y^T(\zeta) \cdot \boldsymbol{R}_z^T(\xi) \tag{8}$$

The cosine of angle χ between $\boldsymbol{n}$ and $\boldsymbol{t}$ reads

$$\cos\chi = \boldsymbol{n} \cdot \boldsymbol{t} = \boldsymbol{n} \cdot \boldsymbol{R} \cdot \boldsymbol{n} = \boldsymbol{R} : (\boldsymbol{n} \otimes \boldsymbol{n}) = \boldsymbol{R} : \boldsymbol{N} \tag{9}$$

where the second order tensor $\boldsymbol{N}$ is according to Kuhl et al. [4] defined as $\boldsymbol{N} = \boldsymbol{n} \otimes \boldsymbol{n}$. Since no gaps or overlaps exist between the rigid bodies, the volume of the domain is summation over volume of individual mechanical elements

$$V = \sum_e V_e = \sum_e \cos\chi_e \frac{A_e l_e}{3} = \sum_e \boldsymbol{R}_e : \boldsymbol{N}_e \frac{A_e l_e}{3} \tag{10}$$

Note that the volume of individual element is negative whenever $\chi > \pi/2$.

3 TENSOR OF EQUIVALENT ELASTIC CONSTANTS

Let us strain the discrete system in macroscopic sense by constant strain tensor $\boldsymbol{\varepsilon}$. According to [4], it is assumed that all the rotations are zeros and differences in translations are dictated by differences in position

$$\varphi = 0 \qquad\qquad \boldsymbol{u}_b - \boldsymbol{u}_a = \boldsymbol{\varepsilon} \cdot (\boldsymbol{x}_b - \boldsymbol{x}_a) \tag{11}$$

The displacement jump on contact between cells a and b reads

$$\boldsymbol{\Delta} = \boldsymbol{u}_b - \boldsymbol{u}_a = l\boldsymbol{\varepsilon} \cdot \boldsymbol{t} \tag{12}$$

where l and $\boldsymbol{t}$ are length and contact vector belonging to element connecting bodies a and b. The normal and shear strain and stress directly follow

$$e_N = \frac{\boldsymbol{n} \cdot \boldsymbol{\Delta}}{l} = \boldsymbol{n} \cdot \boldsymbol{\varepsilon} \cdot \boldsymbol{t} \qquad\qquad \boldsymbol{e}_T = \frac{\boldsymbol{\Delta}}{l} - e_N \boldsymbol{n} = \boldsymbol{\varepsilon} \cdot \boldsymbol{t} - (\boldsymbol{n} \cdot \boldsymbol{\varepsilon} \cdot \boldsymbol{t})\, \boldsymbol{n} \tag{13}$$

$$s_N = E_0 e_N \qquad\qquad \boldsymbol{s}_T = E_0 \alpha \boldsymbol{e}_T \tag{14}$$

where E_0 is the normal stiffness coefficient and α is the tangential/normal stiffness ratio considered constant in the whole domain.

The virtual work done by single element reads

$$\delta W = Al\,(s_N \delta e_N + \boldsymbol{s}_T \cdot \delta \boldsymbol{e}_T) \tag{15}$$

and summation of individual contributions provides the total virtual work in the discrete system.

Let us now define two additional tensors: the fourth order tensor $\boldsymbol{\mathscr{I}}^{\mathrm{vol}}$ and the third order tensor $\boldsymbol{T}$.

$$\boldsymbol{\mathscr{I}}^{\mathrm{vol}} = \frac{\mathbf{1} \otimes \mathbf{1}}{3} \tag{16}$$

$$\boldsymbol{T} = 3\boldsymbol{n} \cdot \left(\boldsymbol{\mathscr{I}}^{\mathrm{vol}}\right)^{T_{13}} - \boldsymbol{n} \otimes \boldsymbol{n} \otimes \boldsymbol{n} \tag{17}$$

where $\mathbf{1}$ is the identity matrix of size 3. Note that $\boldsymbol{T}$ is different from definition in [4, 1] because the symmetry implied by equality $\boldsymbol{t} = \boldsymbol{n}$ is no longer present. The transposition T_{13} means that dimensions 1 and 3 are swapped. Eq. (13) can be rewritten as

$$e_N = \left(\boldsymbol{N} \cdot \boldsymbol{R}^T\right) : \boldsymbol{\varepsilon} \qquad\qquad \boldsymbol{e}_T = \left(\boldsymbol{T} \cdot \boldsymbol{R}^T\right) : \boldsymbol{\varepsilon} \tag{18}$$

using transposition T of the second order tensor swapping its two dimensions $T = T_{12}$.

The virtual work of single element expressed in Eq. (15) can be rewritten as well

$$\begin{aligned}
\delta W &= Al\,(s_N \delta e_N + \boldsymbol{s}_T \cdot \delta \boldsymbol{e}_T) \\
&= AlE_0 \left(\left[\left(\boldsymbol{N} \cdot \boldsymbol{R}^T\right) : \boldsymbol{\varepsilon}\right] \left[\left(\boldsymbol{N} \cdot \boldsymbol{R}^T\right) : \delta\boldsymbol{\varepsilon}\right] + \alpha \left[\left(\boldsymbol{T} \cdot \boldsymbol{R}^T\right) : \boldsymbol{\varepsilon}\right] \cdot \left[\left(\boldsymbol{T} \cdot \boldsymbol{R}^T\right) : \delta\boldsymbol{\varepsilon}\right]\right) \\
&= AlE_0 \left[\boldsymbol{\varepsilon} : \left(\boldsymbol{R} \cdot \boldsymbol{N} \otimes \boldsymbol{N} \cdot \boldsymbol{R}^T\right)^{T_{12}} : \delta\boldsymbol{\varepsilon} + \alpha\boldsymbol{\varepsilon} : \left(\boldsymbol{R} \cdot \boldsymbol{T}^{T_{13}} \cdot \boldsymbol{T} \cdot \boldsymbol{R}^T\right) : \delta\boldsymbol{\varepsilon}\right] \\
&= AlE_0\boldsymbol{\varepsilon} : \left(\left(\boldsymbol{R} \cdot \boldsymbol{N} \otimes \boldsymbol{N} \cdot \boldsymbol{R}^T\right)^{T_{12}} + \alpha \boldsymbol{R} \cdot \boldsymbol{T}^{T_{13}} \cdot \boldsymbol{T} \cdot \boldsymbol{R}^T\right) : \delta\boldsymbol{\varepsilon} \\
&= AlE_0\boldsymbol{\varepsilon} : (\boldsymbol{\mathscr{N}} + \alpha\boldsymbol{\mathscr{T}}) : \delta\boldsymbol{\varepsilon}
\end{aligned} \tag{19}$$

where

$$\boldsymbol{\mathscr{N}} = \left(\boldsymbol{R}\cdot\boldsymbol{N}\otimes\boldsymbol{N}\cdot\boldsymbol{R}^T\right)^{T_{12}} \qquad \boldsymbol{\mathscr{T}} = \boldsymbol{R}\cdot\boldsymbol{T}^{T_{13}}\cdot\boldsymbol{T}\cdot\boldsymbol{R}^T \tag{20}$$

The total virtual work of reads

$$\delta W^{\mathrm{dis}} = \sum_e \delta W_e = \sum_e A_e l_e E_0 \boldsymbol{\varepsilon} : (\boldsymbol{\mathscr{N}}_e + \alpha\boldsymbol{\mathscr{T}}_e) : \delta\boldsymbol{\varepsilon} \tag{21}$$

The discrete system is now related to equally strained elastic isotropic Boltzmann Boltzmann continuum occupying the same domain of volume V. Stress in the continuum is provided by constitutive equation $\boldsymbol{\sigma} = \boldsymbol{D} : \boldsymbol{\varepsilon}$, where $\boldsymbol{D}$ is fourth order tensor of elastic constants. The virtual work of the continuum is

$$\delta W^{\mathrm{con}} = V\boldsymbol{\sigma} : \delta\boldsymbol{\varepsilon} = V\boldsymbol{\varepsilon} : \boldsymbol{D} : \delta\boldsymbol{\varepsilon} \tag{22}$$

The equivalence of the discrete and continuous system implies equality of virtual works

$$\delta W^{\mathrm{dis}} = \delta W^{\mathrm{con}} \tag{23}$$

Substituting Eqs. (21) and (22) into Eq. (23), expression for tensor of elastic constants is derived

$$\boldsymbol{D} = \left\langle \frac{1}{V}\sum_e A_e l_e E_0 \left(\boldsymbol{\mathscr{N}}_e + \alpha\boldsymbol{\mathscr{T}}_e\right) \right\rangle^{\mathrm{SYM}} \tag{24}$$

The symmetrization is needed because the tensors $\boldsymbol{\mathscr{N}}$ and $\boldsymbol{\mathscr{T}}$ do not posses the symmetries required for Boltzmann continuum, which are the *major* symmetry (derived from equivalence of mixed derivatives of elastic potential) and the *minor* symmetry (derived from symmetry of stress and strain tensors). The symmetric part can be easily obtained using transposition T_{34}.

$$\langle\bullet\rangle^{\mathrm{SYM}} = \frac{\bullet + \bullet^{T_{34}}}{2} \tag{25}$$

Thanks to assumed statistical independence between normal and contact vector and elemental area and length, the summation in Eq. (24) can be broken into the following expression

$$\boldsymbol{D} = \frac{E_0}{V}\left\langle \mathrm{E}\left[\boldsymbol{\mathscr{N}}\right] + \alpha\mathrm{E}\left[\boldsymbol{\mathscr{T}}\right]\right\rangle^{\mathrm{SYM}} \sum_e A_e l_e \tag{26}$$

where $\mathrm{E}\left[\bullet(\boldsymbol{x})\right]$ is the mean value of function $\bullet$ dependent on vector $\boldsymbol{x}$ with distribution function $f_{\boldsymbol{X}}(\boldsymbol{x})$

$$\mathrm{E}\left[\bullet(\boldsymbol{x})\right] = \int_{-\infty}^{\infty}\cdots\int_{-\infty}^{\infty} \bullet(\boldsymbol{x}) f_{\boldsymbol{X}}(\boldsymbol{x})\,\mathrm{d}\boldsymbol{x} \tag{27}$$

Substituting V from Eq. (10) and utilizing the statistical independence again, one obtains

$$\boldsymbol{D} = \frac{3E_0}{\mathrm{E}[\boldsymbol{R} : \boldsymbol{N}]}\left\langle \mathrm{E}\left[\boldsymbol{\mathscr{N}}\right] + \alpha\mathrm{E}\left[\boldsymbol{\mathscr{T}}\right]\right\rangle^{\mathrm{SYM}} \tag{28}$$

4 EVALUATION OF EXPECTATIONS

The integration of mean values from Eq. (28) is tedious. It was analytically done in [5] in two dimensions over two independent variable. For three dimensions it has to be performed over four independent angles and the integration cannot be separated since rotation matrix $\boldsymbol{R}$ depends on all four angles. The calculation was performed by computer with a help of Python library for symbolic mathematics SymPy [6]. The following three integrations were delivered.

$$\mathrm{E}\left[\boldsymbol{R}:\boldsymbol{N}\right] = \int_{-\gamma}^{\gamma}\int_{0}^{2\pi}\int_{0}^{\pi}\int_{0}^{2\pi} \boldsymbol{R}:\boldsymbol{N}\frac{1}{2\pi}\frac{\sin\zeta}{2}\frac{1}{2\pi}\frac{\sin\chi}{1-\cos\gamma}\,\mathrm{d}\xi\,\mathrm{d}\zeta\,\mathrm{d}\theta\,\mathrm{d}\chi = \cos^2\left(\frac{g}{2}\right) \tag{29}$$

$$\begin{aligned}\mathrm{E}\left[\boldsymbol{\mathcal{N}}\right] =& \int_{-\gamma}^{\gamma}\int_{0}^{2\pi}\int_{0}^{\pi}\int_{0}^{2\pi} \boldsymbol{\mathcal{N}}\frac{1}{2\pi}\frac{\sin\zeta}{2}\frac{1}{2\pi}\frac{\sin\chi}{1-\cos\gamma}\,\mathrm{d}\xi\,\mathrm{d}\zeta\,\mathrm{d}\theta\,\mathrm{d}\chi = \\ =& \frac{1}{3}\left(\boldsymbol{\mathcal{I}}^{\mathrm{vol}}\right)^{T_{23}} + \frac{2\cos\gamma+\cos 2\gamma+1}{20}\left(\boldsymbol{\mathcal{I}}^{\mathrm{vol}} + \left(\boldsymbol{\mathcal{I}}^{\mathrm{vol}}\right)^{T_{24}} - \frac{2}{3}\left(\boldsymbol{\mathcal{I}}^{\mathrm{vol}}\right)^{T_{23}}\right)\end{aligned} \tag{30}$$

$$\begin{aligned}\mathrm{E}\left[\boldsymbol{\mathcal{T}}\right] =& \int_{-\gamma}^{\gamma}\int_{0}^{2\pi}\int_{0}^{\pi}\int_{0}^{2\pi} \boldsymbol{\mathcal{T}}\frac{1}{2\pi}\frac{\sin\zeta}{2}\frac{1}{2\pi}\frac{\sin\chi}{1-\cos\gamma}\,\mathrm{d}\xi\,\mathrm{d}\zeta\,\mathrm{d}\theta\,\mathrm{d}\chi = \\ =& \frac{2}{3}\left(\boldsymbol{\mathcal{I}}^{\mathrm{vol}}\right)^{T_{24}} - \frac{2\cos\gamma+\cos 2\gamma+1}{20}\left(\boldsymbol{\mathcal{I}}^{\mathrm{vol}} + \left(\boldsymbol{\mathcal{I}}^{\mathrm{vol}}\right)^{T_{23}} - \frac{2}{3}\left(\boldsymbol{\mathcal{I}}^{\mathrm{vol}}\right)^{T_{24}}\right)\end{aligned} \tag{31}$$

Only the symmetric parts of these expectations are needed (Eq. 25). The symmetric parts of involved tensors are

$$\left\langle\left(\boldsymbol{\mathcal{I}}^{\mathrm{vol}}\right)^{T_{23}}\right\rangle^{\mathrm{SYM}} = \left\langle\left(\boldsymbol{\mathcal{I}}^{\mathrm{vol}}\right)^{T_{24}}\right\rangle^{\mathrm{SYM}} = \frac{\boldsymbol{\mathcal{I}}}{3} \tag{32}$$

where the fourth order tensor $\boldsymbol{\mathcal{I}} = \mathcal{I}_{ijkl} = (\delta_{ik}\delta_{jl} + \delta_{il}\delta_{jk})/2$ with $\delta_{ij} \equiv \mathbf{1}$ being the Kronecker delta is employed. The symmetric part of expectations reads

$$\left\langle\mathrm{E}\left[\boldsymbol{\mathcal{N}}\right]\right\rangle^{\mathrm{SYM}} = \frac{2\cos\gamma+\cos 2\gamma+21}{180}\boldsymbol{\mathcal{I}} + \frac{2\cos\gamma+\cos 2\gamma+1}{20}\boldsymbol{\mathcal{I}}^{\mathrm{vol}} \tag{33}$$

$$\left\langle\mathrm{E}\left[\boldsymbol{\mathcal{T}}\right]\right\rangle^{\mathrm{SYM}} = \frac{39-2\cos\gamma-\cos 2\gamma}{180}\boldsymbol{\mathcal{I}} - \frac{2\cos\gamma+\cos 2\gamma+1}{20}\boldsymbol{\mathcal{I}}^{\mathrm{vol}} \tag{34}$$

5 MACROSCOPIC ELASTIC CHARACTERISTICS

The mechanical behavior of linearly elastic isotropic solid is determined by two independent constants (here we choose elastic modulus E and Poisson's ratio ν) defining tensor of elastic constants

$$\boldsymbol{D} = \frac{E}{1+\nu}\boldsymbol{\mathcal{I}} + \frac{3E\nu}{(1+\nu)(1-2\nu)}\boldsymbol{\mathcal{I}}^{\mathrm{vol}} \tag{35}$$

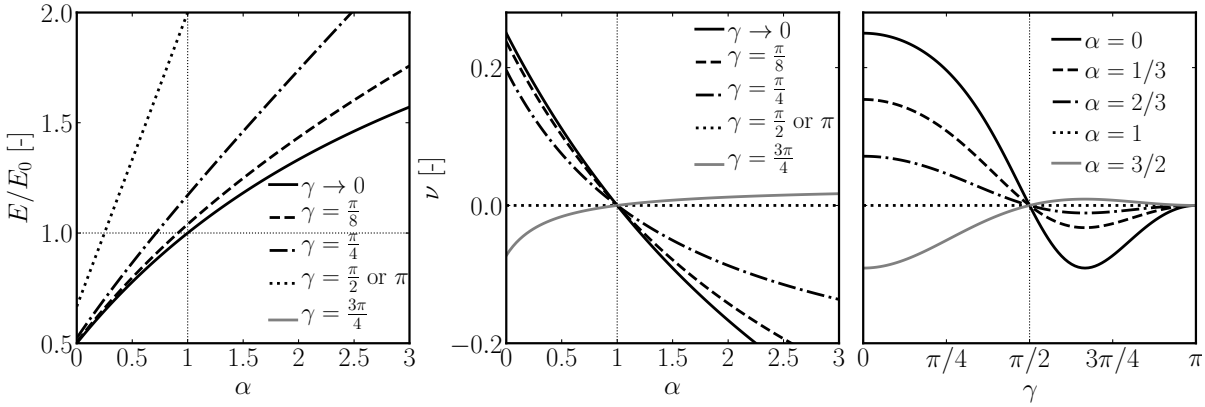

Figure 2: Macroscopic elastic characteristics according to Eqs. (38) and (37).

Equation (28) along with symmetrized expectations (29), (33) and (34) provides

$$\boldsymbol{D} = E_0 \left[\frac{(1-\alpha)(2\cos\gamma + \cos(2\gamma) - 39) + 60}{30(\cos\gamma + 1)} \boldsymbol{\mathscr{I}} + \frac{3(1-\alpha)}{5} \cos\gamma \boldsymbol{\mathscr{I}}^{\mathrm{vol}} \right] \tag{36}$$

Equality between respective scalar multipliers of tensors $\boldsymbol{\mathscr{I}}^{\mathrm{vol}}$ and $\boldsymbol{\mathscr{I}}$ in Eqs. (36) and (35) provides relations between macroscopic parameters E and ν and mesoscopic parameters E_0, α and γ.

$$\nu = \frac{3(1-\alpha)(\cos\gamma + \cos^2(\gamma))}{(1-\alpha)(7\cos\gamma + 7\cos^2\gamma - 20) + 30} \tag{37}$$

$$E = E_0 \frac{2\left[(1-\alpha)(\cos\gamma + \cos^2\gamma - 20) + 30\right]\left[(1-\alpha)(\cos\gamma + \cos^2\gamma - 2) + 3\right]}{(1-\alpha)(7\cos\gamma + 7\cos^2\gamma - 20) + 30} \tag{38}$$

These equations are plotted in Fig. 2 for range $\alpha \in (0, 3)$.

Calculation limit for $\gamma \to 0$ must yield relations for discrete system with $\boldsymbol{n} = \boldsymbol{t}$.

$$\lim_{\gamma\to 0} \nu = \frac{1-\alpha}{4+\alpha} \qquad\qquad \lim_{\gamma\to 0} E = E_0 \frac{2+3\alpha}{4+\alpha} \tag{39}$$

Indeed, the calculation of limits provides correct expressions derived in e.g. [1] under assumption of perpendicularity of contact vector and contact face. They are also identical to those from microplane theory [7].

By differentiate the expression with respect to γ and search for stationary point, the maximum and minimum possible values of Poisson's ratio can be found. The stationary points are $\gamma = 0$, π and $\arccos(-0.5)$ (≈ 2.09440). Plotting the Poisson's ratio with respect to the limit angle γ (Fig. 2 on the right hand side) shows that the maximum range of ν is obtained for $\gamma = 0$, i.e. when the contact vector equals the normal vector. This is the classic solution stated in Eq. (39). Increasing γ towards $\pi/2$ shrinks the interval of achievable Poisson's ratios to zero. The interval opens again beyond $\pi/2$ with opposite signs; its width maximizes at $\gamma = \arccos(-0.5)$. The limiting values at this point are obtained at $\alpha = 0$ and $\alpha \to \infty$ as $(-0.091, 0.034)$. The maximum values of Poisson's ratio are achieved for $\boldsymbol{n} = \boldsymbol{t}$, any deviation of the model geometry from this relation causes narrowing of the Poisson's ratio limits.

6 CONCLUSIONS

- It has been proven that under assumption (5) one cannot increase the Poisson's ratio limits beyond what is provided by model with $\boldsymbol{n} = \boldsymbol{t}$ in Eq. (39).
- The formulas are derived from strong and unrealistic assumption about rotations and displacements in the model (Eq. 11). Behavior of the real model will be less rigid, however the overall effect on macroscopic elastic constants should be qualitatively the same.
- The same conclusions were found for 2D models under the same assumptions in [5].
- The theory will be extended to arbitrary distribution of χ and verified by comparison with real behavior of discrete systems.

ACKNOWLEDGEMENT

Financial support provided by the Czech Science Foundation under project No. GA19-12197S is gratefully acknowledged.

REFERENCES

[1] Jan Eliáš. Boundary layer effect on behavior of discrete models. *Materials*, 10:157, 2017. ISSN 1996-1944. doi:10.3390/ma10020157.

[2] Peter Grassl and John E. Bolander. Three-dimensional network model for coupling of fracture and mass transport in quasi-brittle geomaterials. *Materials*, 9(9):782, 2016. ISSN 1996-1944. doi:10.3390/ma9090782.

[3] John E. Bolander and Shigehiko Saito. Fracture analyses using spring networks with random geometry. *Engineering Fracture Mechanics*, 61(5-6):569–591, 1998. ISSN 0013-7944. doi:10.1016/S0013-7944(98)00069-1.

[4] Ellen Kuhl, Gian Antonio D'Addetta, Hans J. Herrmann, and Ekkehard Ramm. A comparison of discrete granular material models with continuous microplane formulations. *Granular Matter*, 2(3):113–121, 2000. ISSN 1434-5021. doi:10.1007/s100350050003.

[5] Jan Eliáš. On macroscopic elastic properties of isotropic discrete systems: effect of tessellation geometry. In *Proceedings of the Tenth International Conference on Fracture Mechanics of Concrete and Concrete Structures - FraMCoS-X held in Bayonne, France*, 2019.

[6] Aaron Meurer, Christopher P. Smith, Mateusz Paprocki, Ondřej Čertík, Sergey B. Kirpichev, Matthew Rocklin, AMiT Kumar, Sergiu Ivanov, Jason K. Moore, Sartaj Singh, Thilina Rathnayake, Sean Vig, Brian E. Granger, Richard P. Muller, Francesco Bonazzi, Harsh Gupta, Shivam Vats, Fredrik Johansson, Fabian Pedregosa, Matthew J. Curry, Andy R. Terrel, Štěpán Roučka, Ashutosh Saboo, Isuru Fernando,

Sumith Kulal, Robert Cimrman, and Anthony Scopatz. Sympy: symbolic computing in Python. *PeerJ Computer Science*, 3:e103, 2017. ISSN 2376-5992. doi:10.7717/peerj-cs.103.

[7] Ignacio Carol and Zdeněk P. Bažant. Damage and plasticity in microplane theory. *International Journal of Solids and Structures*, 34(29):3807–3835, 1997. ISSN 0020-7683. doi:10.1016/S0020-7683(96)00238-7.